

The effect of the symmetrical deformation $y = x^{k+1}$ on the optimization of the symmetrical multiple channeled white light color filter

ZINA BARAKET*, JIHENE ZAGHDOUDI, MOUNIR KANZARI

The Photovoltaic and Semiconductor Materials Laboratory, El-Manar University-ENIT,
P.O. Box 37, Le Belvedere, 1002-Tunis, Tunisia

*Corresponding author: baraket.zina@yahoo.fr

In this paper, we consider a hybrid photonic crystal symmetrically deformed ($Bg_5/Cu_3/Bg_5$) consisting of the third generation of the copper mean sequence (Cu_3), sandwiched between two Bragg mirrors at the fifth generation (Bg_5). Our system realizes a polychromatic filter that transmits five wavelengths in the visible spectrum independently of the polarization of the light transverse electric or transverse magnetic. Secondly, the photonic crystal ($Bg_5/Cu_3/Bg_5$) undergoes the deformation $y = x^{k+1}$ (where k is the degree of deformation, x and y are respectively the coordinates of the system before and after the deformation). With a proper choice of the degree of deformation k , this photonic crystal maintains its property of polychromatic filter whose transmission wavelength is independent of the polarization's state. Thanks to this deformation, we can disperse the optical windows in different spectra of visible light and exactly in the violet, blue, green, and orange light. This system can be used in the fabrication of color filter devices and the white light emitting diodes.

Keywords: photonic crystals, symmetry, filter, polarization, optimization.

1. Introduction

The study of one-dimensional photonic crystals is the subject of several research projects over the past decades. The fundamental property of a 1D photonic crystal is the existence of forbidden frequencies regions called a photonic band gap that allows the realization of novel materials. Besides, a deeper knowledge of the behaviors of the photonic crystals permits us to create novel systems for photonic applications. The existence of defects confirms the presence of sharp peaks in the transmission spectrum. Generally, in the far field of photonic crystals applications the focus lies on asymmetrically chirped structures such as the omnidirectional reflectors [1]. The investigation of the behavior of the defects allows the improvement of the performance of the filters [2]. Some literature reported that multiple channeled filters based on chirped photonic crystals cover essentially the microwave and infrared regions. Contrarily, the multiple color filters that allow the propagation of transverse electric (TE) and transverse magnetic (TM)

modes at oblique incidence and covering the visible range are rarely investigated [3]. One of the most primordial features of 1D photonic crystals filters is the tenability of the photonic band gap and the resonant defect modes. Besides, the transmission of light through photonics crystals is affected by both the geometric and computational parameters [4, 5]. Thus the tunable resonant modes can be realized by the symmetrical chirping of geometrical thickness of the layers.

From this point of view and based on the transfer matrix method, we analyze the optical properties of the hybrid symmetrically chirped photonic crystal ($Bg_5/Cu_3/Bg_5$) consisting of the third generation of the quasi-periodic copper mean sequence Cu_3 inserted between two Bragg mirrors Bg_5 at the fifth generation. Also, due to the symmetrical chirping, we will be able to disperse the resonant modes in different spectra of visible light.

We consider the simple copper mean multilayers which are composed of two building blocks H and L and arranged according to the subsequent recursive relationships [6, 7]

$$S_{j+1} = S_{j-1}^2 S_j, \quad j > 2$$

with $S_0 = L$, $S_1 = H$, and S_j is the j -th generation of the copper mean sequence. The symmetrical copper mean sequence is obtained as the method described in [8, 9]. The Bragg sequence Bg_n is arranged as $(LH)^n H$.

The study is structured as follows: in the next section we present a brief summary of the transfer matrix method. Section 3 is devoted to the results of numerical simulation and discussion while the conclusions are summarized in Section 4 [10].

2. Simulation method

The TMM approach technique is a finite difference method particularly well suited to the analysis of PBG materials and widely used for the description of optical properties of the stacked layers [11, 12].

Furthermore, Abeles proves that the amplitudes of the incident electric field E_0^+ , the reflected electric field E_0^- and the transmitted wave after m layers E_{m+1}^+ are related by the following matrix [11, 12]:

$$\begin{bmatrix} E_0^+ \\ E_0^- \end{bmatrix} = C_1 C_2 C_3 C_m \begin{bmatrix} E_{m+1}^+ \\ E_{m+1}^- \end{bmatrix}$$

here C_m is the well-known transfer matrix whose elements are

$$C_m = \begin{pmatrix} \frac{\exp(-i\varphi_m)}{t_m} & \frac{r_m \exp(i\varphi_m)}{t_m} \\ \frac{r_m \exp(-i\varphi_m)}{t_m} & \frac{\exp(i\varphi_m)}{t_m} \end{pmatrix}$$

where φ_m is the phase shift between the layers m and $m + 1$ and t_m, t_r are the Fresnel reflection and the transmission coefficient. It should be mentioned that the phase φ_m is extremely dependent on any deformation of the multilayers.

Let us note y as the coordinates of the system after deformation that may be connected to x , the coordinates of the initial system according to the subsequent function $y = x^{k+1}$, where k is the degree of the deformation. In the absence of any deformation we talk about the initial phase which can be expressed as [1]:

$$\varphi_m = \frac{2\pi}{\lambda} x_0 \cos(\theta_m) \quad \text{with} \quad x_0 = \frac{\lambda_0}{4}$$

After the deformation the phase shift between the layers m and $m + 1$ becomes

$$\varphi_m = \frac{2\pi}{\lambda} x_0 \left[m^{k+1} - (m-1)^{k+1} \right] \cos(\theta_m)$$

Then, we calculate the transmittance of energy T for both of polarization s and p :

$$T_s = \text{Re} \left[\frac{n_{m+1} \cos(\theta_{m+1})}{n_0 \cos(\theta_0)} \right] |t_s|^2$$

$$T_p = \text{Re} \left[\frac{n_{m+1} \cos(\theta_{m+1})}{n_0 \cos(\theta_0)} \right] |t_p|^2$$

3. Results and discussion

For the numerical simulation of the transmittance of the above-mentioned photonic crystal in the visible range of wavelengths, we select the TiO_2 and SiO_2 as two dielectric materials with high and low indices of refraction, respectively, $n_H = 2.3$ and $n_L = 1.45$. The dielectric materials are assumed to be isotropic, linear, non-absorbing and with no optical activity. The geometrical thickness of both kinds of layers (d_H, d_L) is taken to form quarter wave stack such as $n_H d_H = n_L d_L = \lambda_0/4$ with $\lambda_0 = 0.5 \mu\text{m}$ as the reference wavelength [13]. The focus lies on the analysis of the symmetrical photonic crystal constructed by using the copper mean quasi-periodic photonic crystal intercalated between two periodic photonic crystals. We supposed that the incident medium is the air with refractive index $n_0 = 1$ as well the glass is used as a substrate with refractive index $n_s = 1.5$. We consider both the TE and TM polarized waves in our calculations. Figures 1 and 2 explicit the optical response of our system in 3D and 2D, respectively. We perceive the realization of a polychromatic filter within which the positions of the optical windows depend on the incident angle for TE and TM polarizations.

As depicted in Fig. 2 we remark that the TM and TE modes behave similarly at normal incidence but when the angle of incidence increases, the width of the peaks becomes larger for the TM mode than in the TE mode. We should note that the defect modes and the band gap have shifted to the small wavelengths as the incident angle

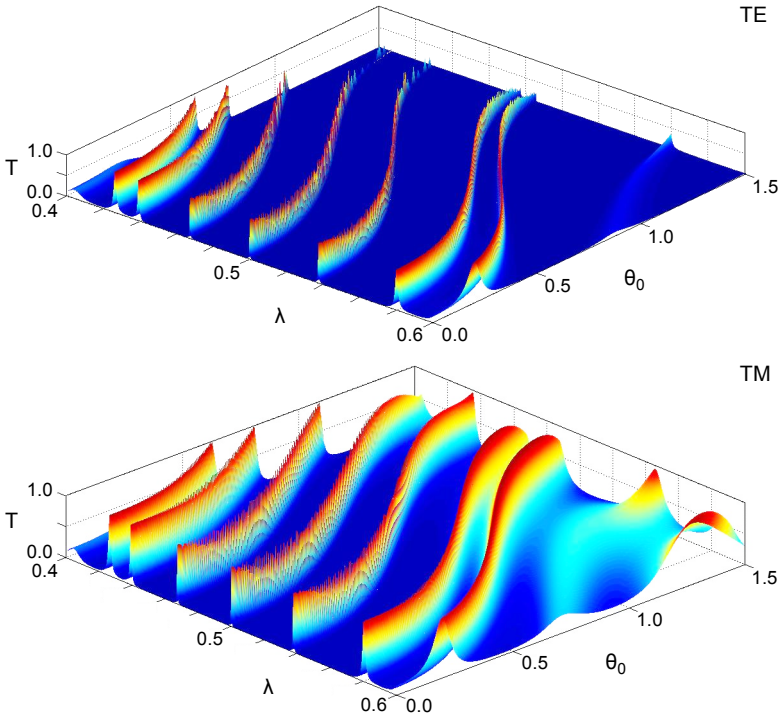


Fig. 1. The 3D transmittance spectra of the system ($Bg_5/Cu_3/Bg_5$) for the polarization TE and TM.

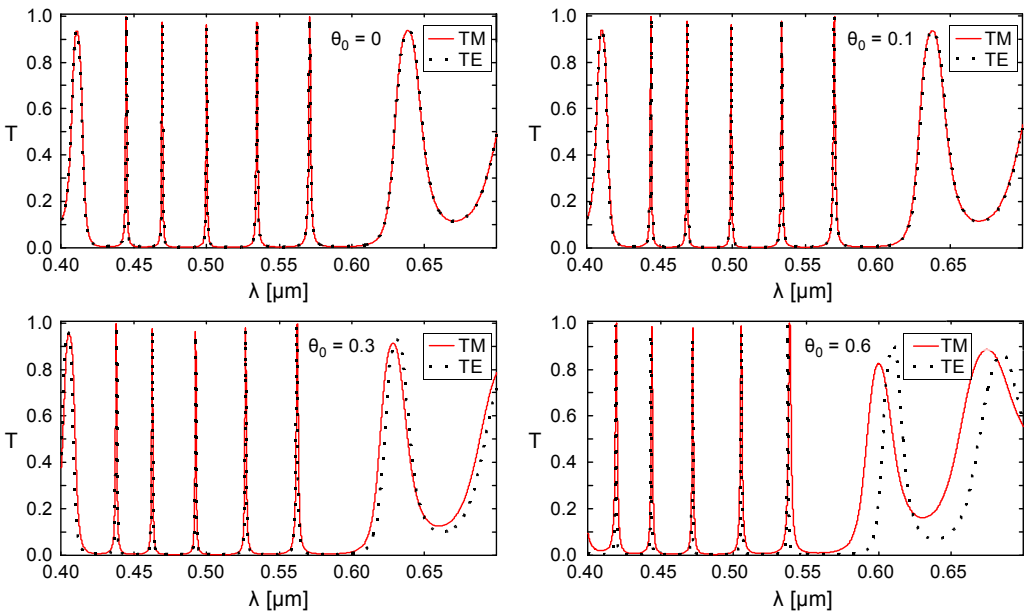


Fig. 2. The transmittance spectra of the symmetrical photonic crystal ($Bg_5/Cu_3/Bg_5$) for different incident angle.

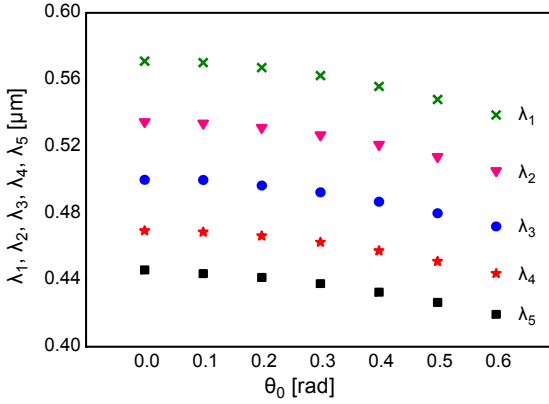


Fig. 3. The variation of the position of the peaks *versus* the incident angle.

increases for the TM and TE polarized waves. This displacement is well-known as the blue shift [14]. So, the defect modes and band gaps are very strongly dependent on the incident angle and polarizations.

Also we can perceive that the photonic crystal acts as a polychromatic filter. The positions of peaks are invariant for the two polarizations as long as the incident angle is less than 0.6 rad. We are able to filter the same wavelengths for the two polarizations.

In addition, we express in Fig. 3 the variation of the positions of the peaks as a function of the angle of incidence. The positions of the peaks as a function of θ_0 verify a polynomial law of fourth degree

$$\lambda_i = a_i + b_i \theta_0 + c_i \theta_0^2 + d_i \theta_0^3 + m_i \theta_0^4$$

where λ_i (in micrometers) is the wavelength of the peak, a_i, b_i, c_i, d_i and m_i are constants depending of each peak.

We seek to improve the performance of the filter. For this reason we apply symmetrically the deformation designed by $y = x^{k+1}$, where x and y are the coordinates of the system before and after the deformation, and k is the deformation degree as presented in Fig. 4.

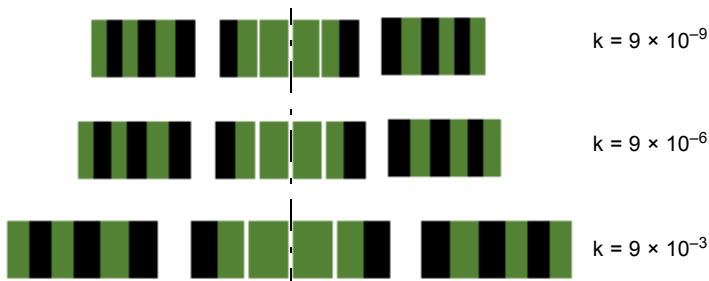


Fig. 4. Symmetrical deformed 1D photonic crystal with different degree of deformation $k = 9 \times 10^{-9}$, $k = 9 \times 10^{-6}$, and $k = 9 \times 10^{-3}$.

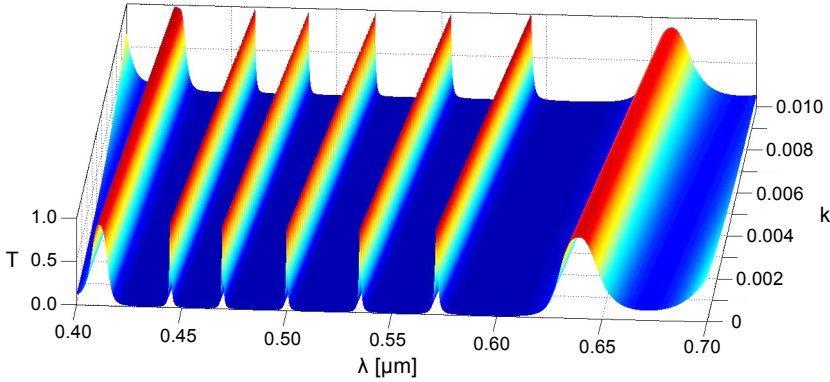


Fig. 5. The transmittance spectrum of the deformed photonic crystal $Bg_5/Cu_3/Bg_5$ versus k and λ at the normal incidence.

Figure 5 shows the optical response of the system as a function of k and λ .

The defined deformation allows the enlargement of the geometrical thickness of the layers when k increases. Consequently, as k rises, the optical thickness of each layer increases and the wavelength confined in the cavities becomes larger.

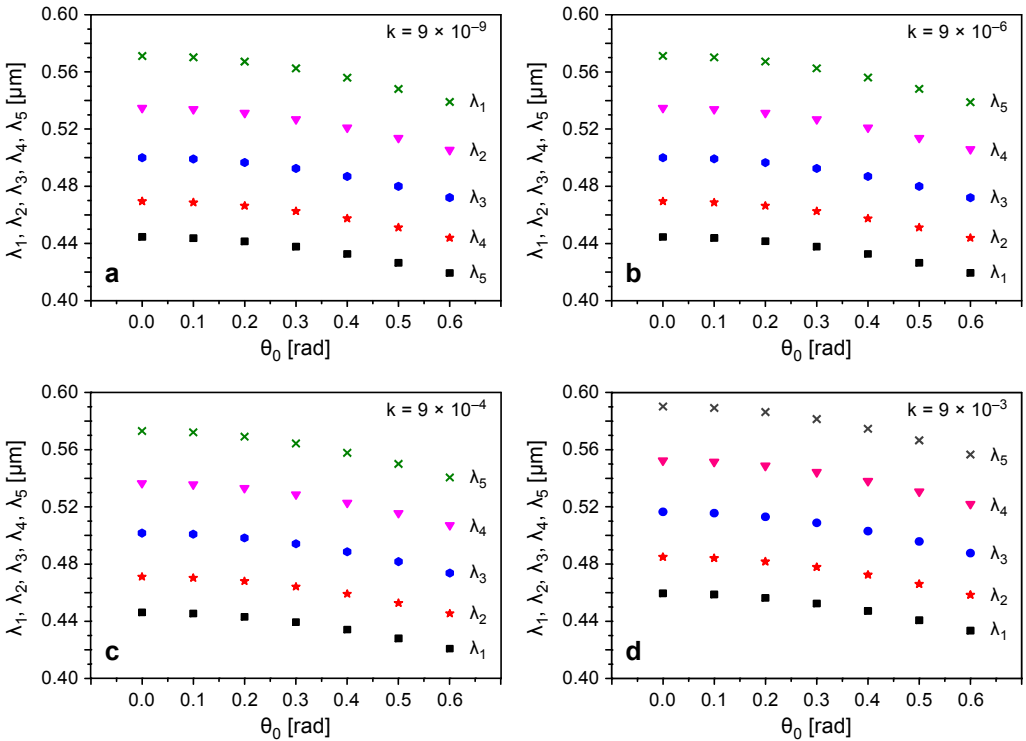


Fig. 6. Position of the peaks versus the incident angle for different degree of deformation: $k = 9 \times 10^{-9}$ (a), $k = 9 \times 10^{-6}$ (b), $k = 9 \times 10^{-4}$ (c) and $k = 9 \times 10^{-3}$ (d).

Therefore, it is important to note that $\lambda_1, \lambda_2, \lambda_3, \lambda_4$, and λ_5 are the wavelengths localized in the cavities of the system. According to the Bragg condition, the confined wavelength λ_{peak} must verify that $nd = m\lambda_{\text{peak}}/2$ where nd is the optical thickness of the cavity at normal incidence and m is an integer [15].

Figure 6 illustrates the optical response of the system $\text{Bg}_5/\text{Cu}_3/\text{Bg}_5$ for a different value of k .

Figures 6a–6d show the variation of the positions of the peaks as a function of the incident angle for four different values of k . The property of the independence of the polarization is observed again. We highlight a displacement of the positions of the peaks to the higher wavelengths also called a red shift.

By observing the behavior of the wavelength λ_5 in Fig. 6d, we detect a displacement of the position of the peak from $0.571 \mu\text{m}$ when $k = 0$ to $0.5904 \mu\text{m}$ when $k = 9 \times 10^{-3}$ at normal incidence. A similar behavior is obtained for the wavelengths $\lambda_1, \lambda_2, \lambda_3, \lambda_4$.

An interesting application of the symmetrical deformation is the construction of a filter whose optical windows are distributed in the various spectra of the white light and covering the spectra of violet, blue, green, and orange light. Let's take the case of our filter in the absence of deformation ($k = 0$) at normal incidence that enables the transmission of wavelengths $\lambda_1, \lambda_2, \lambda_3, \lambda_4$, and λ_5 which respectively belong to the spectra of green, green, blue and violet light. Indeed, when k is equal to 9×10^{-3} , the deformed photonic crystal can localize the wavelengths $\lambda_1, \lambda_2, \lambda_3, \lambda_4$, and λ_5 respectively in the violet, blue, green, and orange light. The equations which control the positions of the optical windows as a function of θ_0 , when k reaches 9×10^{-3} , are as follows:

$$\lambda_1 = (45.96 + 0.152\theta_0 - 8.867\theta_0^2 + 2.045\theta_0^3 + 0.379\theta_0^4) \times 10^{-2}$$

$$\lambda_2 = (48.5 - 0.0295\theta_0 - 0.0764\theta_0^2 - 0.01591\theta_0^3 + 0.03409\theta_0^4) \times 10^{-2}$$

$$\lambda_3 = (51.66 + 0.08896\theta_0 - 9.352\theta_0^2 + 1.136\theta_0^3 + 1.136\theta_0^4) \times 10^{-2}$$

$$\lambda_4 = (55.24 + 0.207\theta_0 - 10.186\theta_0^2 + 1.692\theta_0^3 + 1.136\theta_0^4) \times 10^{-2}$$

$$\lambda_5 = (59.04 - 0.0607\theta_0 - 9.542\theta_0^2 - 2.5\theta_0^3 + 4.167\theta_0^4) \times 10^{-2}$$

In order to investigate extensively the characteristics of the filter, we must study the behavior of the bandwidth of the filter when the degree of deformation k increases. The Figure 7 shows the transmission peak of each wavelength for both $k = 0$ and $k = 3 \times 10^{-9}$.

The value of the deformation degree k must be taken very small in order to avoid the displacement of the position of the peak and we can compare the bandwidth of the filter with the case $k = 0$. As can be seen in Fig. 7, the width of each transmission peak $\lambda_1, \lambda_2, \lambda_3, \lambda_4$, and λ_5 is constant when the deformation degree k increases and reaches precisely $k = 3 \times 10^{-9}$.

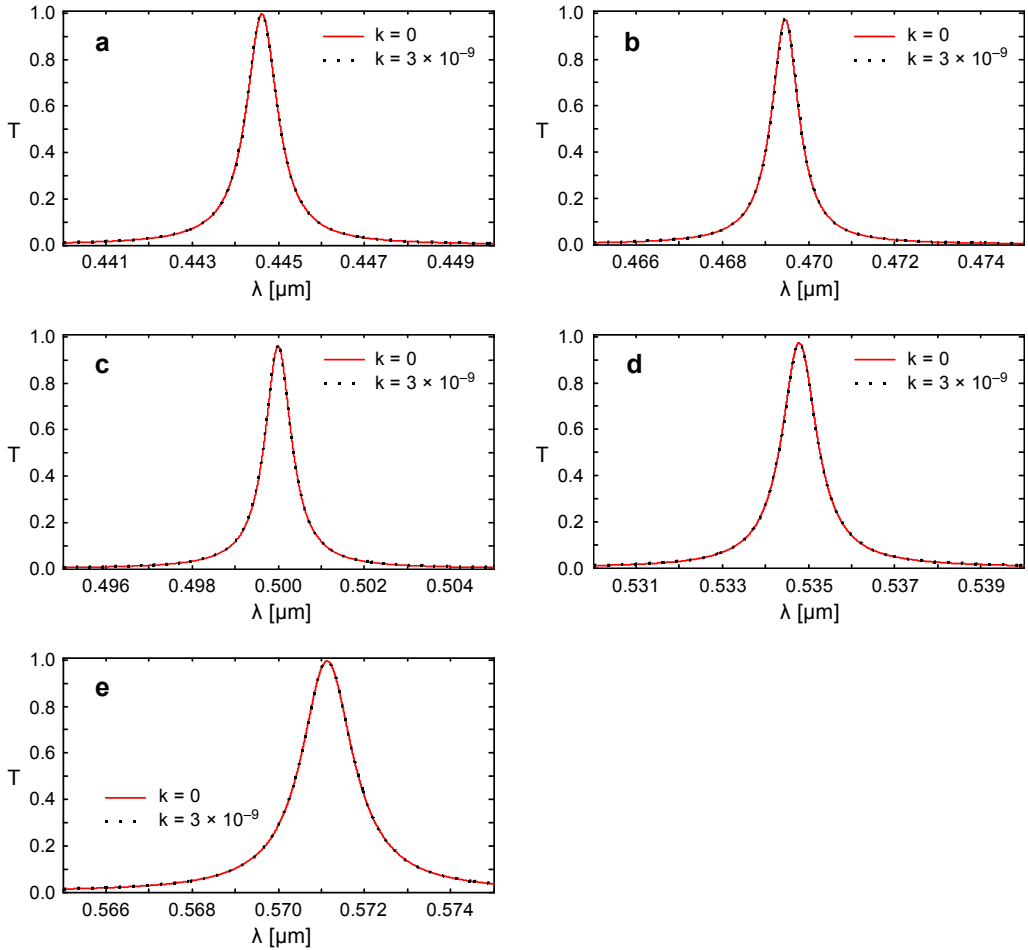


Fig. 7. The transmission peak at normal incidence for different wavelength λ_1 (a), λ_2 (b), λ_3 (c), λ_4 (d), and λ_5 (e) for $k=0$ and $k=3 \times 10^{-9}$.

Now, let the deformation degree k rise and attain $k=3 \times 10^{-6}$. Figure 8 represents the five transmission peaks when $k=0$ and $k=3 \times 10^{-6}$.

The photonic crystals behave as in the previous case and the bandwidth of the filter remains unchanged. We conclude that the symmetrical deformation $y=x^{k+1}$ saves the bandwidth of the filter when k increases. The theoretical analysis of the optical response of the system $\text{Bg}_5/\text{Cu}_3/\text{Bg}_5$ gives helpful information for the designing and the manufacturing of a tunable filter [14].

The polychromatic filters covering the white light are not abundant compared to the infrared and microwave ranges. As well, the system allows the transmission of five wavelengths which represents a powerful optimization of the filter cited in [16] that

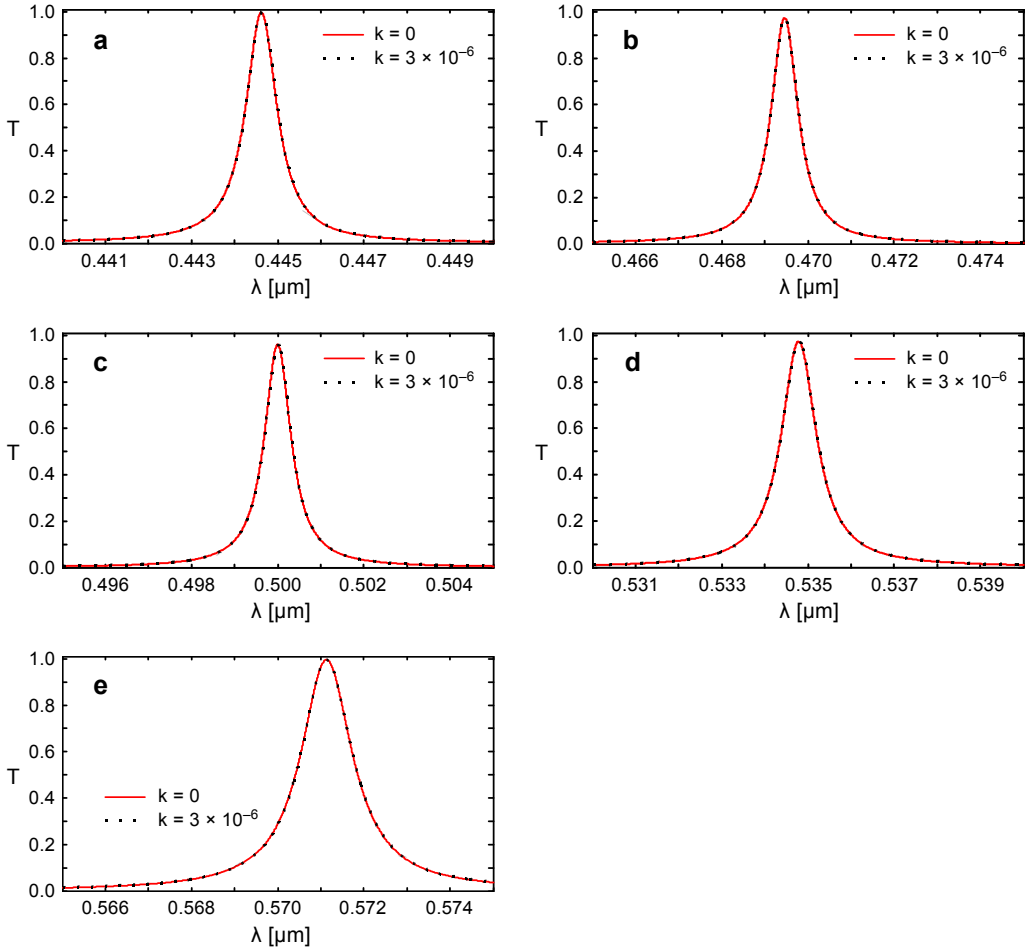


Fig. 8. The transmission peak at normal incidence for different wavelength λ_1 (a), λ_2 (b), λ_3 (c), λ_4 (d), and λ_5 (e) for $k=0$ and $k=3 \times 10^{-6}$.

simply permits the transmission of only three wavelengths in the visible range. Taking these results into consideration, we can make more practical tunable filters [14]. Therefore, it is important to advertise that our system can be exploited in the engineering of white light emitting diode devices (LED).

4. Conclusion

In summary, the symmetrical photonic crystal $\text{Bg}_5/\text{Cu}_3/\text{Bg}_5$ realizes a polychromatic filter with five peaks where the positions of the peaks are independent of the nature of the polarization TE or TM. Due to the symmetrical deformation, we can ameliorate

the performance of the filter by assuring the distribution of the positions of the peaks in a different range of visible light. This primordial property allows us to use the system in the fabrication of color filter devices and white light emitting diodes (LED).

References

- [1] MOULDI A., KANZARI M., *Design of an omnidirectional mirror using one dimensional photonic crystal with graded geometric layers thicknesses*, *Optik – International Journal for Light and Electron Optics* **123**(2), 2012, pp. 125–131.
- [2] TZU-CHYANG KING, CHIEN-JANG WU, *Properties of defect modes in one dimensional symmetric defective photonic crystals*, *Physica E: Low-dimensional Systems and Nanostructures* **69**, 2015, pp. 39–46.
- [3] HUIHUAN GUAN, PEIDE HAN, YUPING LI, HONGWEI ZHOU, XUE ZHANG, RUIZHEN ZHANG, *Optimization of dichromatic filters based on photonic heterostructures of Si/MgF₂*, *Optics Communications* **285**(10–11), 2012, pp. 2656–2659.
- [4] XING XIAO, WANG WENJUN, LI SHUHONG, ZHENG WANQUAN, ZHANG DONG, DU QIANQIAN, GAO XUOXI, ZHANG BINGYUAN, *Investigation of defect modes with Al₂O₃ and TiO₂ in one-dimensional photonic crystals*, *Optik – International Journal for Light and Electron Optics* **127**(1), 2016, pp. 135–138.
- [5] HONG WANG, GUANGJUN WANG, YANLING HAN, YONGTAO WANG, *Tunable double-channel filter based on defect mode splitting of one-dimensional magnetic photonic crystal*, *Optics Communications* **285**(21–22), 2012, pp. 4558–4561.
- [6] YUPING ZHANG, ZHIXIN WU, YANYAN CAO, HUIYUN ZHANG, *Optical properties of one-dimensional Fibonacci quasi-periodic graphene photonic crystal*, *Optics Communications* **338**, 2015, pp. 168–173.
- [7] DE SPINADE V.W., *New smarandache sequences: the family of metallic means*, *Smarandache: Notions Journal* **8**, 1997, p. 81.
- [8] COELHO I.P., VASCONCELOS M.S., BEZERRA C.G., *Effects of mirror symmetry on the transmission fingerprints of quasiperiodic photonic multilayers*, *Physics Letters A* **374**(13–14), 2010, pp. 1574–1578.
- [9] BARAKET Z., ZAGHDOUDI J., KANZARI M., *Study of optical responses in hybrid symmetrical quasi-periodic photonic crystals*, *Progress in Electromagnetics Research M (PIER M)* **46**, 2016, pp. 29–37.
- [10] ARAÚJO C.A.A., VASCONCELOS M.S., MAURIZ P.W., ALBUQUERQUE E.L., *Omnidirectional band gaps in quasiperiodic photonic crystals in the THz region*, *Optical Materials* **35**(1), 2012, pp. 18–24.
- [11] YEH P., YARIV A., *Optical Waves in Crystals: Propagation and Control of Laser Radiation*, Wiley, New York, 1984, p. 589.
- [12] TRABELSI Y., BOUZZI Y., BENALI N., KANZARI M., *Narrow stop band optical filter using one-dimensional regular Fibonacci/Rudin Shapiro photonic quasicrystals*, *Optical and Quantum Electronics* **48**(1), 2016, article ID 54.
- [13] SINGH B.K., THAPA K.B., PANDEY P.C., *Optical reflectance and omnidirectional bandgaps in Fibonacci quasicrystals type 1-D multilayer structures containing exponentially graded material*, *Optics Communications* **297**, 2013, pp. 65–73.
- [14] BARATI M., AGHAJAMALI A., *Near-infrared tunable narrow filter properties in a 1D photonic crystal containing semiconductor metamaterial photonic quantum-well defect*, *Physica E: Low-dimensional Systems and Nanostructures* **79**, 2016, pp. 20–25.
- [15] MENEZ L., ZAQUINE I., MARUANI A., FREY R., *Experimental investigation of intracavity Bragg gratings*, *Optics Letters* **27**(7), 2002, pp. 479–481.
- [16] HONGFEI LI, HUIHUAN GUAN, PEIDE HAN, YUPING LI, CAILI ZHANG, *Design for abroad non-transmission band gap of three-color filters using photonic heterostructures*, *Optics Communications* **287**, 2013, pp. 162–166.

*Received April 6, 2016
in revised form June 12, 2016*